Effects of colonization, luminescence, and autoinducer on host transcription during development of the squid-vibrio association

Carlene K. Chun*†, Joshua V. Troll*, Irina Koroleva‡§, Bartley Brown¶, Liliana Manzella‡‖, Einat Snir‡, Hakeem Almabrazi¶, Todd E. Scheetz**, Maria de Fatima Bonaldo‡‖, Thomas L. Casavant¶, M. Bento Soares‡‖, Edward G. Ruby*, and Margaret J. McFall-Ngai*††

*Department of Medical Microbiology and Immunology, University of Wisconsin, Madison, WI 53706; and Departments of ‡Pediatrics, **Ophthalmology and Visual Science, and ¶Electrical and Computer Engineering, University of Iowa, Iowa City, IA 52242

Edited by Nancy A. Moran, University of Arizona, Tucson, AZ, and approved May 8, 2008 (received for review March 9, 2008)

The light–organ symbiosis between the squid *Euprymna scolopes* and the luminous bacterium *Vibrio fischeri* offers the opportunity to decipher the hour-by-hour events that occur during the natural colonization of an animal's epithelial surface by its microbial partners. To determine the genetic basis of these events, a glass-slide microarray was used to characterize the light-organ transcriptome of juvenile squid in response to the initiation of symbiosis. Patterns of gene expression were compared between animals not exposed to the symbiont, exposed to the wild-type symbiont, or exposed to a mutant symbiont defective in either of two key characters of this association: bacterial luminescence or autoinducer (AI) production. Hundreds of genes were differentially regulated as a result of symbiosis initiation, and a hierarchy existed in the magnitude of the host's response to three symbiont features: bacterial presence > luminescence > AI production. Putative host receptors for bacterial surface molecules known to induce squid development are up-regulated by symbiont light production, suggesting that bioluminescence plays a key role in preparing the host for bacteria-induced development. Further, because the transcriptional response of tissues exposed to AI in the natural context (i.e., with the symbionts) differed from that to AI alone, the presence of the bacteria potentiates the role of quorum signals in symbiosis. Comparison of these microarray data with those from other symbioses, such as germ-free/conventionalized mice and zebrafish, revealed a set of shared genes that may represent a core set of ancient host responses conserved throughout animal evolution.

Euprymna | fischeri | microarray | symbiosis

Among the most common beneficial microbial associations are those between bacteria and the host epithelia they colonize. In many associations, a complex program of tissue adaptation and development is triggered by the presence of the symbionts (1–3); however, the nature of these programs and how they lead to the initiation of persistent beneficial relationships are poorly understood. Such knowledge is a vital part of understanding both how animals achieve a healthy state and how an invasion by pathogens compromises its maintenance. To address these questions, biologists are using a variety of vertebrate and invertebrate model systems that each reveals insights into a different aspect of host–bacteria interaction, such as cell–cell signaling, development, and immune response (4–10). Comparative studies among these various associations have had three broad goals: (*i*) to determine traits that are shared across the animal kingdom, (*ii*) to identify the factors driving the diversification of specific symbioses, and (*iii*) to define the principal differences between how the host interacts with a beneficial partner and with a pathogen. Recent progress toward these goals has followed technological advances on a number of fronts, including the creation of bioinformatics tools for inferring the composition and activities of a host's microbial partners (11, 12). In addition, genome-wide analyses of host gene expression during the development of an association have revealed the number and identities of genes that are differentially regulated in the formation of a successful, stable interaction at the epithelium–bacteria interface (5, 13).

The symbiotic association between the Hawaiian squid *Euprymna scolopes* and the luminous bacterium *Vibrio fischeri* has served as a useful model to analyze the onset and maintenance of a natural host–microbe relationship (10, 14). In this association, *V. fischeri* occurs as a monoculture growing along the apical surfaces of the epithelia that line crypts located deep within the squid's light-emitting organ. The nascent light organ of a newly hatched juvenile squid is free of symbionts (or "aposymbiotic") and, while being exposed to the hundreds of bacterial species present in seawater, becomes colonized only by *V. fischeri*. Despite this specificity, the association is initiated within minutes of hatching as bacteria within the seawater begin to gather in host-derived mucus shed by the superficial epithelia of the organ. Three to four hours later the amassed *V. fischeri* cells migrate to pores on the organ's surface, travel up cilia-lined ducts, and enter the blind-ended crypts. Interaction with the bacteria also induces development of host tissues: most notably, at ≈12 h after inoculation, the symbionts trigger the irreversible loss of the superficial epithelium (Fig. 1), with which they are not in direct contact. The regression of this epithelium involves a series of events, including the trafficking of macrophage-like cells into the tissue, apoptosis of the epithelial cells, and an eventual sloughing of these cells. This extensive morphogenesis is mediated by molecules released by the symbionts, including the lipid A component of LPS and the tetrapeptide monomer of peptidoglycan (PGN), two derivatives of the bacterial cell envelope (10, 14). In addition, the symbionts induce changes in the host cells with which they directly associate (Fig. 1); specifically, they induce a swelling of the crypt epithelial cells and an increase in the density of their microvilli (10).

Author contributions: C.K.C., J.V.T., I.K., M.d.F.B., M.B.S., E.G.R., and M.J.M.-N. designed research; C.K.C., J.V.T., I.K., L.M., E.S., and M.d.F.B. performed research; B.B., H.A., T.E.S., T.L.C., and M.B.S. contributed new reagents/analytic tools; C.K.C., J.V.T., I.K., B.B., H.A., T.E.S., M.d.F.B., T.L.C., M.B.S., E.G.R., and M.J.M.-N. analyzed data; and C.K.C., E.G.R., and M.J.M.-N. wrote the paper.

The authors declare no conflict of interest.

This article is a PNAS Direct Submission.

Data deposition: All sequences are publicly available on the Sanger Institute Database (www.sanger.ac.uk/DataSearch). The 3-prime sequences have been submitted to the GenBank Database (accession nos. DW251302–DW286722).

†Present address: Stanford University Medical School, Stanford, CA 94305.

§Present address: Novartis Institutes for Biomedical Research, Inc., Cambridge, MA 02139.

‖Present address: Children's Memorial Research Center, Northwestern University, Chicago, IL 60614.

††To whom correspondence should be addressed. E-mail: mjmcfallngai@wisc.edu.

This article contains supporting information online at www.pnas.org/cgi/content/full/0802369105/DCSupplemental.

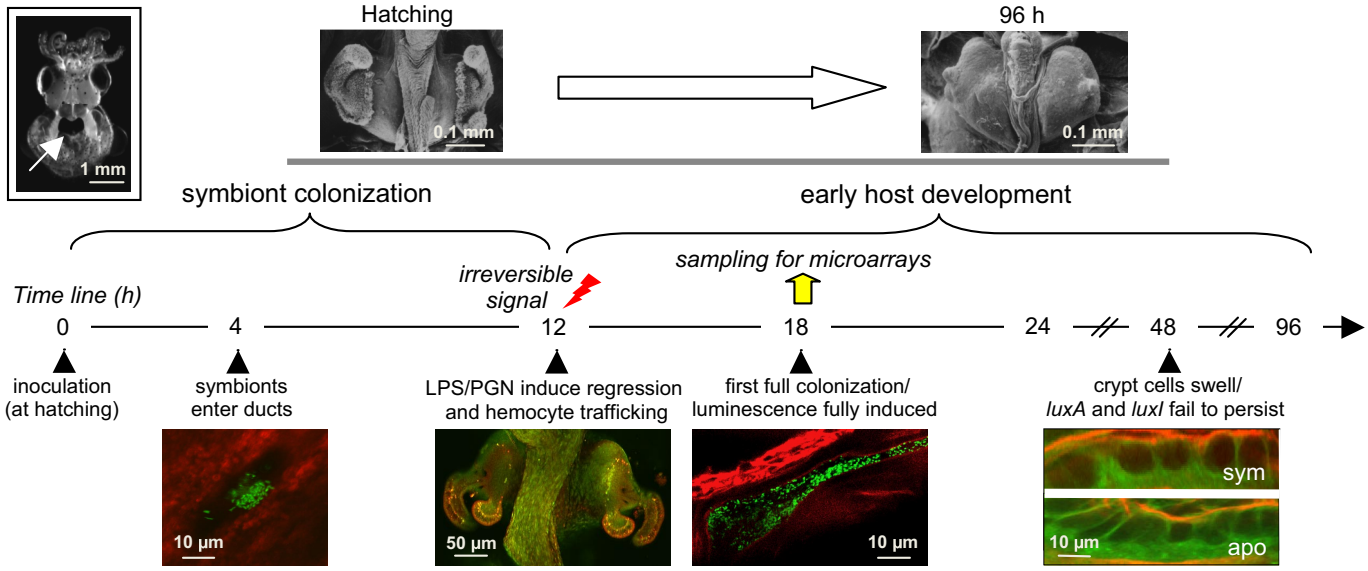

Fig. 1. Features of early host development in the squid-vibrio symbiosis. The light-organ tissues undergo a series of symbiont-induced developmental events (see text for details), here visualized by scanning electron microscopy (*Upper*) and confocal microscopy (*Lower*). After aggregating in host mucus, at 4 h, GFP-labeled *V. fischeri* cells (green) enter host tissues (red). At 12 h, the symbionts induce the loss of the superficial ciliated epithelium that facilitates colonization, a process that is complete by 96 h. By 18 h, the time when host transcriptional responses were characterized, bacteria fill the epithelium-lined crypts (red) and are highly luminous. By 48 h, symbionts induce crypt-cell swelling, a phenotype that is not observed in colonizations by *luxA* and *luxI* mutants, and that correlates with their inability to persist.

In this symbiosis, the only known contribution of the bacteria is luminescence (15), which is mediated by quorum signaling, a cell–cell sensing mechanism by which beneficial and pathogenic bacterial species coordinately control gene expression in a cell-density-dependent manner (16). *V. fischeri* cells do not induce luminescence until ≈8 h after inoculation. By then, the accumulation of the second of two *V. fischeri*-produced quorum signals (17), the 3-oxohexanoyl-L-homoserine lactone autoinducer (AI) molecule, leads to the full induction of the lux operon, which encodes the light-emitting enzyme subunits of luciferase (LuxA and LuxB) and the AI synthase (LuxI) (18). The ability to produce both luciferase and AI is critical to the symbiosis; mutants defective in either of these factors fail to induce crypt cell swelling or to persist normally in the light organ beyond 24 h. Interestingly, colonization by a *luxA* (but not a *luxI*) mutant additionally fails to induce either proper hemocyte trafficking or regression of the superficial epithelium (19). This differential response may reflect that (*i*) the *luxA* mutant (unlike the *luxI*) produces AI, and/or (*ii*) the *luxI* mutant (unlike the *luxA*) still produces a small amount of luminescence (18). Thus, to fully understand the mechanisms that trigger these developmental events (Fig. 1), we must determine how each of these two consequences of symbiotic colonization, luminescence and AI production, differentially affects the host.

We hypothesized that the dramatic developmental events that occur in response to colonization would be reflected in underlying transcriptional changes in host light-organ tissues. The recent construction of an *E. scolopes* light-organ-derived EST database, consisting of a set of 13,962 unique sequences (20), led to the design of a glass-slide microarray for the study of global changes in host-gene expression during symbiosis. We used this microarray to characterize and separate the host's transcriptional response to the presence of three components of the symbiosis: bacterial symbionts, luminescence, and AI. Patterns of light-organ gene expression were determined 18 h after inoculation of juvenile squid, when all of the conspicuous symbiont-induced developmental programs have been triggered, and the bacterial partners have fully colonized the organ and are producing maximal levels of luminescence.

Results

Hierarchical Host Transcriptional Responses to Symbiont Colonization. To reveal broad patterns of gene expression that result from interaction with the symbiont, we analyzed eight individual comparisons of colonization treatments, as well as three comparisons of larger groupings of general colonization conditions, or "grouped conditions": with/without symbionts, with/without luminescence, or with/without AI (Table 1). All comparisons were based on four independent biological replicates of each colonization treatment [see supporting information (SI) *Text* for details]. Two lines of evidence support a hierarchy among the grouped conditions; bacterial presence itself had the greatest effect, followed by symbiont light production, and then AI production. This evidence includes: (*i*) the topology of a microarray condition tree (Fig. 2), which was derived from the expression levels of 781 differentially regulated genes in all individual comparisons of colonization treatments; and (*ii*) the frequency and patterns of differential gene regulation in individual and specific grouped conditions (Tables 1, 2, S1, and S2). In addition, the reliability of these microarray expression results was confirmed by quantitative real-time PCR (QRT-PCR) analysis (*SI Text*). Nine of the 10 genes analyzed were differentially regulated in both the same direction and magnitude as predicted from the array data (Table S3).

Analysis of the Condition Tree. To examine the overall clustering of the gene expression data among treatments, we created a condition tree (Fig. 2) based on the average expression values ($n = 3$) of the 781 unique differentially expressed transcripts in the individual comparisons (Tables 1 and S4). The two aposymbiotic conditions (Apo and Apo + AI) clustered separately from all of the symbiotic conditions. They also clustered separately from each other, indicating that the transcriptional profile is significantly affected by AI addition, even in the absence of symbionts. The transcriptional profiles of all symbiotic light organs clustered together. However, organs not exposed to luminescence (i.e., animals colonized by the *luxA* mutant) had expression profiles that clustered separately from those that were exposed. Based on this indication of the impact of luminescence, we predicted that the transcriptional profile derived

Table 1. Numbers of light-organ transcripts differentially regulated between conditions

Comparisons	Total number of transcripts*	Number of transcripts differentially regulated ≥ 2-fold						
		Total	Up†	Down†	Known‡	Unknown/Hypo‡	No hits‡	Expression class§
Grouped conditions¶								
Symbionts vs. no symbionts	132	70	33	37	42	8/8	12	N
Light vs. no light	27	19	15	4	9	5/2	3	P
AI vs. no AI	10	10	10	0	5	3/1	1	O
Individual conditions								
Wild type vs. apo	462	262	141	121	145	45/31	41	A, B, D, E
Wild type vs. *luxA*	211	149	96	53	57	54/1	37	D, E, F, G
Wild type vs. *luxI*	131	99	50	49	37	36/0	26	B, C, E, F
Wild type vs. *luxI* + AI	24	24	9	15	8	2/12	2	Q
Apo vs. apo + AI	13	2	2	0	1	1/0	0	H
Apo vs. *luxI*	154	94	57	37	56	17/9	12	K, L
Apo + AI vs. *luxI* + AI	148	89	55	34	51	16/9	13	L, M
luxI vs. *luxI* + AI	32	16	11	5	5	1/5	5	I, J

*Transcripts significantly differentially regulated between conditions (see *Methods*); total number of unique transcripts for all grouped conditions, 145; total number for all individual conditions, 781.

†Those transcripts up- or down-regulated ≥2-fold, calculated as the first condition over the second.

‡Known, related to a described gene; unknown/hypo, undescribed or hypothetical protein; no hits, no significant homology to the nonredundant database of Genbank, as determined by BLASTX analysis.

§Letter designation indicates the expression class in Fig. S1 and/or Table S5.

¶Differences between conditions sharing the same category of exposure condition. "Symbiont" includes wild type, *luxI*, *luxI* + AI and *luxA*; "no symbiont" includes apo and apo + AI; "light" includes wild type, *luxI* + AI; "no light" includes apo, apo + AI and *luxA*; "AI" includes wild type, apo + AI, *luxI* + AI and *luxA*; and, "no AI" includes apo and *luxI*.

from *luxI* + AI (bright luminescence) would more closely resemble that of wild type (bright) than that of *luxI* (dim) (18). However, the individual profiles of light organs colonized by *V. fischeri* producing any luminescence (wild type, *luxI*, and *luxI* + AI) did not resolve with high confidence (Fig. 2). Two conclusions arise from these data: (*i*) even the low levels of light emission produced by the *luxI* mutant are sufficient to trigger much of the host's symbiotic response to luminescence, and (*ii*) the presence of luminescence has a greater influence on the transcriptional profile of the juvenile light organ than does the presence or absence of AI.

Frequency and Patterns of Differential Gene Regulation. The relative number (Table 1), as well as the fold change (Tables 2 and S2), of differentially regulated transcripts among the grouped conditions

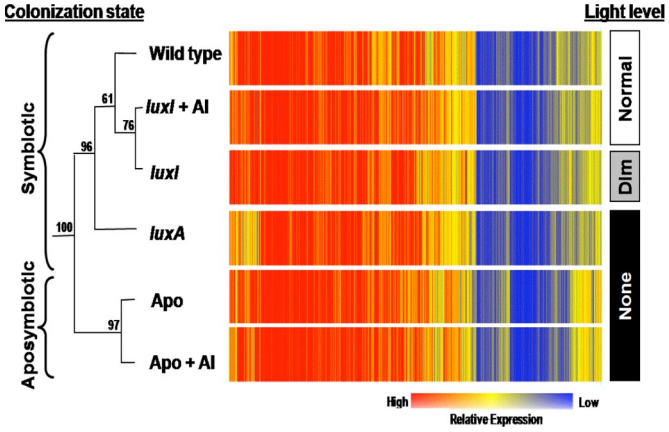

Fig. 2. Transcriptional profiles of light organs exposed to different colonization conditions. Juvenile squid were either left uninoculated (apo) or inoculated with wild-type, *luxA*, or *luxI* strains of *V. fischeri*, in the presence or absence of added AI. The relative similarities of patterns of gene expression under the different conditions were mapped by using change correlation average linkage. Numbers at the nodes represent percent confidence from bootstrapping analysis (n = 1,000). The relative levels of luminescence produced in the light organs under each condition are also indicated.

was also consistent with the dominance hierarchy of: the presence of bacteria > luminescence > AI. This hierarchical relationship was further supported by a three-way Venn diagram comparison, in which we characterized the patterns of differential gene expression during *V. fischeri* colonization with (*i*) both luminescence and AI present (wild type vs. Apo), (*ii*) luminescence present but no AI (wild type vs. *luxI*), and (*iii*) AI present but no luminescence (wild type vs. *luxA*) (Fig. S1*A* and Table S5 *A–G*).

We also did two pair-wise comparisons to determine the influence of colonization state on responses to AI. We first compared {Apo vs. Apo + AI} with {*luxI* vs. *luxI* + AI} to assay the effects of AI irrespective of colonization (Fig. S1*B*; Table S5 *H–J*). If the presence of the bacterial colonization were not required for the light organ to respond to AI, we would expect a similar result from these two comparisons. However, more than twice the number of transcripts were differentially regulated when AI was added in the presence of *V. fischeri* cells than in their absence, and only one transcript, annotated as "unknown," was shared. Therefore, the host tissue naturally responds to the presence of AI only in the biologically relevant condition of the presence of symbionts. This tissue response may work indirectly through the activity of AI on another bacterial activity(s). The second pair-wise comparison, {Apo vs. *luxI*} and {Apo + AI vs.

Table 2. Transcripts regulated by all three conditions

Annotation of transcript	Fold change*		
	S/NS	L/NL	A/NA
Require symbionts with luminescence and AI			
LPS-binding protein	8.6	4.4	3.4
Peptidoglycan recognition protein 1	7.3	4.7	2.2
Galaxin-1 (unknown function)	4.8	3.3	2.6
Galaxin-2 (unknown function)	4.1	2.9	2.2
Tetraspanin 3 (membrane trafficking)	2.2	1.9	1.5

Complete list in Table S2, including transcripts regulated by only one or two of the conditions

*Calculated as the first condition relative to the second; S/NS, symbionts vs. no symbionts; L/NL, light vs. no light; or A/NA, AI vs. no AI (e.g., Table 1).

MICROBIOLOGY

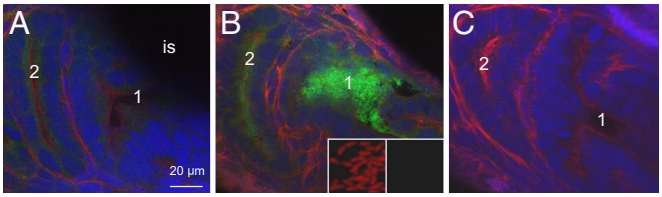

Fig. 3. Localization of EsLBP in juvenile light-organ crypts using confocal immunocytochemistry (ICC) (36). (*A*) In aposymbiotic animals, FITC-labeled secondary antibodies localized EsLBP (green) to the apical surfaces of the crypt epithelia. (*B*) In symbiotic animals, the epithelia remained labeled; however, a large amount of labeling had appeared in the crypt spaces as well. The staining was not the result of *V. fischeri* cells directly binding the EsLBP antibody. (*Inset*) When these bacteria (≈1 μm), counterstained with propidium iodide (red; *Left* of *Inset*), were treated with the EsLBP antibody, there was no binding (*Right*). (*C*) Preimmune controls of both aposymbiotic and symbiotic crypts showed no nonspecific staining. In all images, counterstaining of animal tissues included TOTO3 (blue), which labels nucleic acids; and rhodamine phalloidin (red), which labels filamentous actin. Numbering indicates the two largest of the three crypts in each image; ''is'' indicates the ink sac. See details in *SI Text*.

luxI + AI} (Fig. S1*C*; Table S5 *K–M*) allowed an analysis of the effect of AI on the light organ's transcriptional response to the presence (or absence) of a bacterial colonization. There was an 80% overlap in the identity of the differentially regulated genes, reinforcing the notion that the presence of the bacteria is the most significant driving force in the alteration of gene expression during symbiosis. We were unable to perform a similarly detailed analysis of the role of luminescence, because it was not technically feasible to introduce light to the crypt epithelium in the absence of symbionts.

Regulation of Specific Genes and Response Pathways. The presence of the symbiont and the production of luminescence were expression classes with patterns of gene regulation of particular interest. Approximately one-third of the transcripts regulated solely by the presence of symbionts were either directly associated with signal-transduction pathways (13%) or were transcription factors (20%) (Table S5*A*). Of special significance was the differential regulation of transcripts encoding proteins typically associated with the responses of animals to bacterial infection. These proteins include receptors and other components of immune-related response systems, such as the NF-kappaB and MAP-kinase pathways (21), as well as components of the Kruppel-like factor regulatory cascade (22). For example, the presence of symbionts up-regulates genes encoding a putative host LPS-binding protein [*E. scolopes* LBP or EsLBP (20)] and PGN-recognition proteins (EsPGRP1 and EsPGRP2), as well as elements of both the NF-kappaB pathway (I-kappaB, I-kappaB kinase-gamma, and I-kappaB-zeta variant 3) and its associated proteasome-ubiquitin pathway (e.g., proteasome subunits, ubiquitin ligases, cullin-3). Because derivatives of LPS and PGN act as symbiont-derived morphogens that trigger host development (14), it is not surprising that expression of the putative receptors for these ligands, as well as components of their downstream response pathways, are regulated by the presence of bacterial colonization. To investigate whether such differential gene regulation would correspond to changes in encoded-protein production, we localized EsLBP within juvenile tissues in response to symbiont colonization (Fig. 3). The pattern of cross-reactivity of antibodies to this protein was markedly different between 18-h apo- and symbiotic animals in two ways. First, under either condition, antibody labeling occurred along the apical surfaces of the crypt epithelia; however, in symbiotic animals, strong labeling was also present within the crypt spaces that housed the colonizing symbionts. Second, the overall amount of labeling in the tissues was greater in symbiotic animals, correlating to the increased transcription of EsLBP (Tables 2 and S3).

In contrast to the above-described patterns of gene up-regulation, many transcripts encoding orthologs of proteins involved in the synthesis and maintenance of ciliated surfaces (e.g., orthologs of dynein isoforms and of rootletin) were down-regulated in response to the presence of symbionts. This decrease in transcript level occurs concomitantly with a major developmental event: the bacteria-triggered loss of the light organ's superficial ciliated epithelium (10), a structure that plays an important role in the initial stages of colonization. Interestingly, several transcripts that are likely to encode proteins associated with the visual transduction cascade (e.g., orthologs of the eye-specific retinal-binding protein, guanylate cyclase-1, and guanylate cyclase activator 1A) were also differentially regulated. The expression of these genes, as well as other orthologs encoding proteins of visual transduction, in the tissues of the juvenile light organ was first reported in the recent analyses of the *E. scolopes* EST database (20) and may indicate a mechanism by which the light organ perceives the level of bacterial luminescence. These microarray results suggest that the expression of the visual transduction transcripts is a response to the presence of symbionts and not a direct response to their luminescence, because the regulation was similar between juveniles colonized by the wild type and the nonluminous *luxA* mutant.

In addition to these effects of the presence of the symbionts, the Venn diagram analyses indicated that luminescence specifically induces the differential regulation of a number of host genes (Fig. S1*A*). One transcript, encoding the oxygen-carrying blood pigment hemocyanin (23), exhibited a remarkable pattern of differential regulation that suggests a clear significance to the symbiosis. The levels of hemocyanin transcript appear the same in both aposymbiotic animals and animals colonized by wild-type *V. fischeri* (Table S5*G*); however, animals colonized by the *luxA* mutant showed a dramatic down-regulation in hemocyanin transcript level. These data suggest that, when colonized by a nonluminous mutant of *V. fischeri*, the host responds by reducing the transport, and perhaps availability, of oxygen in the light organ, thereby sanctioning a defective symbiont (18).

Shared Symbiont-Induced Genes Among Animal Hosts. Whereas global gene regulation in the host during pathogenesis has been extensively documented (reviewed in ref. 24), there are only a few studies of the responses of animal tissues to interactions with beneficial microbial partners (5, 13, 25, 26). Gordon and coworkers (5) have previously determined that 59 differentially regulated transcripts of known annotation are shared between two distantly related vertebrates, zebrafish and mouse, in studies of the response of the gut epithelia to colonization by their normal microbiota. Of these 59 transcripts, the EST database of the squid light organ contains 45 genes that are either orthologs or in a shared gene family (Table S6). Our BLASTX analyses suggest that the other 14 genes are specific to vertebrates and their relatives. Interestingly, 16 of the 45 transcripts (5 orthologs and 11 in a shared gene family) were also differentially regulated among the 462 transcripts expressed differently between symbiotic and aposymbiotic light organs (Tables S4, S6, and S7). This differential regulation of the shared genes is highly significant ($P = 3.3 \times 10^{-7}$ by Fisher's Exact test; $P = 1.2 \times 10^{-10}$ by χ^2 test) (*SI Text*). Recent studies of the host transcriptome changes in *Yersinia enterocolitica* pathogenesis (27) have similarly demonstrated differential regulation of several of these genes (Table S7).

Discussion

Host Transcriptional Responses to Colonization by Wild-Type, *luxA*, and *luxI* Symbionts. Unique to this study is the comparison of host responses to either wild-type symbionts or isogenic symbionts defective in characters known to be essential for a persistent symbiosis, i.e., light production (*luxA*) and AI quorum sensing

(*luxI*) (18). The differences in induction of host transcriptional responses shared by these two mutants compared to wild-type symbionts (Fig. S1) are likely to reflect those genes involved in regulating events like crypt cell swelling and bacterial persistence, phenotypes that are defective in both these mutants (18). In contrast, the greater extent of host differential gene regulation in the *luxA* compared to the *luxI* mutant (Table S1) is likely to reflect host phenotypes like hemocyte trafficking and regression of the superficial epithelial field that are defective only in the *luxA* mutant (19). The different timing of the onset of these host phenotypes (Fig. 1) may correlate to the presence or absence of luminescence in the two mutants (Fig. 2).

How might differences in the host's transcriptional response to the *luxA* mutant underlie the inability of this strain to trigger normal light-organ morphogenesis? The absence of symbiont luminescence results in a 4- to 5-fold lower level of transcription of a putative LPS-binding protein and a PGN-recognition protein (Table 2). Further research will be required to demonstrate unequivocally that these specific proteins are the receptors for derivatives of *V. fischeri* LPS and PGN. Nevertheless, they are orthologs of receptors that sense these bacterial molecules, which are morphogens that signal light-organ development (10, 14). Thus, symbiont light production, which occurs at low to normal levels in *luxI* and wild-type strains (Fig. 2), appears to be coupled to the induction of receptors for these symbiont signals. These signals would then mediate morphogenesis of the epithelial surface. Such a coupling would provide a feed-forward response to the developing symbiosis. Also, nonluminous symbionts are delayed in triggering light-organ morphogenesis and may be eliminated before they can mediate the complete regression of host tissues that facilitate colonization (10). As such, the animal would remain receptive to inoculation by a subsequent *V. fischeri* strain that is luminescent. Interestingly, the small amount of luminescence of the *luxI* mutant seems to be sufficient to induce aspects of normal early development (e.g., hemocyte trafficking) but does not rescue the persistence defect, which appears later (18). Whether the second *V. fischeri* AI (17) also contributes to the triggering of these (or other) events in host development remains to be determined.

Does the host respond to symbiont light emission itself or to the lowering of the ambient oxygen concentration resulting from the strong oxygenase activity of the luminescent reaction? One hypothesis is that sensory proteins located in the organ (unpublished data) and encoded by orthologs of genes of the visual transduction cascade (20) are involved in the perception of bacterial luminescence, i.e., a direct mechanism to detect the presence of nonluminous "cheaters" (28). Alternatively, a differential regulation of host genes involved in oxygen utilization might indicate that the animal responds to the marked difference in oxygen utilization by wild-type and *luxA* symbionts (28). In regard to the latter hypothesis, it is interesting to note that a dramatic down-regulation of the gene encoding the host's blood pigment, hemocyanin, occurs during colonization by the *luxA* mutant (Tables S3 and S3). Thus, some portions of the host's responses to *luxA* symbionts may reflect a failure to provide normal oxygen levels to the light organ, affecting both tissue development and the bacterial population.

The transcriptional response to AI addition, in the presence or absence of bacterial symbionts, provides evidence that host tissues react differently to this signal molecule depending on whether they are colonized. These data reinforce the idea that the presentation of chemical signals and other effectors in the absence of the natural bacteria–host context can lead to different and potentially misleading molecular responses (27). In the squid-vibrio system, the host's response to AI is quite limited when compared with that evoked by the presence of either the bacteria themselves or their light production (Table S1). Although the small number of genes that are directly regulated by AI may play an important role, this study suggests that quorum signaling is a conversation held principally among the bacterial symbionts and the host's response appears largely to be mediated indirectly, i.e., through the effects of AI on the activities of the colonizing bacteria, such as luminescence. Because little overlap was observed between the genes regulated by luminescence and those regulated by AI (Figs. 2 and S1*A*), the host's perception of a defect in the *luxI* strain is likely to be independent of its attenuated level of light production. Instead, we propose that the differential between the host's response to wild-type and *luxI* symbionts is due to the activities of other, nonlux, *V. fischeri* genes that are regulated by AI (ref. 29; data not shown).

Similar Transcriptional Responses to Bacterial Symbionts Among Different Animal Hosts. The magnitude of the differential transcriptional regulation (i.e., hundreds of genes) that characterizes the interaction of *E. scolopes* with its symbionts is similar to that reported in other microarray studies of both pathogenic and beneficial animal–bacterial interactions (e.g., refs. 5, 13, 27). Thus, the transcriptional studies presented here not only provide a rich dataset that will inform further characterization of the squid-vibrio symbiosis but also add to a growing database defining the genomic responses of host organisms to their bacterial associates, regardless of the nature of the relationship.

The host squid's transcriptional responses identified here offer an opportunity to determine bacteria-induced changes in gene expression that are either specific to, or conserved across, different taxa of the animal kingdom. These shared changes in gene expression and possible functional pathways may represent a core set of host responses to the extracellular colonization of the apical surfaces of polarized epithelia. For example, a closer study of the 16 differentially regulated genes shared in the mouse, zebrafish, and squid symbioses reveal several associated with the immune response, including components involved in the NF-kappaB and oxidative stress pathways (Table S7). These data support the idea that this response, rather than being entirely devoted to self/nonself recognition, is a principal mechanism by which host animals control responses to bacteria, whether they are persistent beneficial partners or harmful pathogens (30, 31). In addition, an examination of the annotated portion of the total 781 differentially regulated transcripts (Table S4) suggests a pivotal role for three transcription factors that may work alone or coordinately in the control of epithelium–bacteria interactions: NF-kappaB, the ETS family, and the Kruppel-like family. ELF3, an ETS-family transcription factor (Table S2), is specific to epithelial cells, and mutations in this gene have been implicated in abnormal development of intestinal epithelia and in cancer (32, 33). Relevant here is that a recent study of host infection by uropathogenic *Escherichia coli* (UPEC) revealed that the gene encoding ELF3 is differentially regulated by the pathogen and suggested a link between epithelial differentiation and the proinflammatory response (34). Similarly, Kruppel-like transcription factors (Table S4) are also implicated in host responses, often mediating bacteria-induced changes in the host cytoskeleton (22, 34). The observation that these three transcription factors are differentially regulated in a wide variety of bacterial associations suggests they and their targets may be essential players in the control of epithelial colonization, regardless of the type of symbiosis.

As in our study, most of the attention to differentially regulated transcripts has in the past focused on genes whose functions can be inferred from annotated orthologs. However, as microarray-based transcriptional information becomes available for other symbiotic systems, a comparison of these databases may reveal certain "hypothetical" genes that commonly respond to bacterial colonization. Such an analysis could identify novel host transcripts that might play a conserved role in the maintenance of beneficial interactions with bacteria.

This study of the patterns of host transcriptional responses in the squid-vibrio symbiosis has produced a wealth of hypothesis-generating information. The data present a "snapshot" view of the host transcriptome at 18 h postinoculation, a critical time in the

trajectory of symbiotic development, and serve as a foundation for future characterizations of the events that precede and follow. As in most other such studies, these results represent an averaging of the transcriptional changes across a set of tissues. A more precise understanding of these changes at the tissue and cellular level will come from the localization of the expression of specific genes and gene-products by *in situ* hybridization and immunocytochemistry (e.g., refs. 35, 36). Such approaches may, for example, reveal that both the crypt epithelia, which are interacting directly with the symbionts, and the superficial epithelia, which are induced to regress (Fig. 1), exhibit significant differences in their patterns of gene expression that reflect the distinct developmental fates of these two tissues.

Whereas by 2005, dozens of microarray studies had been performed to describe host responses to pathogens (24), to date only a few have characterized transcriptional regulation in the interactions of animals with their normal microbiota. Thus, an understanding of genome-wide responses between animals and their coevolved microbial partners is still in its infancy. With the growing awareness that such associations are the most prevalent type of bacteria-host interaction, similar analyses of other systems promises an exciting horizon for the study of how animals and bacteria form and maintain long-term, mutually beneficial alliances.

Methods

Squid Colonization Experiments. Juvenile animals were collected within minutes of hatching and transferred to glass vials containing 2 ml of Hawaiian offshore seawater (HOSW). HOSW contains a natural assemblage of many kinds of marine bacteria, but has an insufficient number of *V. fischeri* to initiate light-organ colonization (10). A subset of juveniles was provided with no *V. fischeri* inoculum, i.e., were maintained aposymbiotic (apo), whereas the rest were made symbiotic by the addition of either wild-type *V. fischeri* ES114 (11), or *luxI* or *luxA* mutants of this strain (18). In all cases, symbiosis was initiated by placing the juveniles in vials containing 1,000 cells of the inoculating strain per milliliter of HOSW. After 6 h, all of the squid were transferred to fresh vials containing 2 ml of uninoculated HOSW; in some treatments, the vials contained an addition of 5 μM synthetic AI (Sigma-Aldrich).

Preparation of Light-Organ Tissues for Microarray Analyses. Six experimental treatments of juvenile animals were performed for the microarray matrix: uncolonized (Apo); uncolonized, but supplemented with AI (Apo + AI); colonized by wild-type *V. fischeri* (wild type); colonized by a mutant defective in luciferase synthesis (*luxA*); colonized by a mutant defective in AI synthesis (*luxI*); and, colonized by the *luxI* mutant, but supplemented with AI (*luxI* + AI) (Figs. 2 and S2 and S3). At 18 h postinoculation, animals were anesthetized in 2% ethanol in HOSW, and the light organs were removed into RNAlater (Ambion Biosystems). See *SI Text* for details.

Microarray Hybridizations and Analyses. Spotted glass microarrays (GLP3825) were prepared from a nonredundant cDNA library containing 13,962 sequences, obtained from 0- to 48-h postinoculation juvenile squid light organs as described (20). Each spotted-array experiment was performed with 1 μg of total RNA. In addition to three biological replicates of the six treatment conditions described above, dye-swap replicates and two on-chip replicates (for a total of at least four technical replicates/treatment) were performed for each treatment condition.

ACKNOWLEDGMENTS. We thank M. Rise for assistance with data analysis and A. Wier for comments on the manuscript. This work was supported by grants from the W. M. Keck Foundation (M.J.M.-N and E.G.R.), by National Institutes of Health (NIH) Grants R01-RR12294 (to E.G.R.) and R01-AI50661 (to M.J.M.-N.), and by National Science Foundation Grants IOS 0517007 (to M.J.M.-N. and E.G.R.) and IOS 0715905 (to M.J.M.-N.). This paper is HIMB contribution no. 1313.

1. McFall-Ngai M (2002) Unseen forces: the influence of bacteria on animal development. *Dev Biol* 242:1–14.
2. Xu J, Gordon J (2003) Honor thy symbionts. *Proc Natl Acad Sci USA* 100:10452–10459.
3. Bates J, *et al.* (2006) Distinct signals from the microbiota promote different aspects of zebrafish gut differentiation. *Dev Biol* 297:374–386.
4. Graf J (2006) Molecular requirements for the colonization of *Hirudo medicinalis* by *Aeromonas veronii*. *Prog Mol Subcell Biol* 41:291–303.
5. Rawls JF, Samuel BS, Gordon JI (2004) Gnotobiotic zebrafish reveal evolutionarily conserved responses to the gut microbiota. *Proc Natl Acad Sci USA* 101:4596–4601.
6. Cheesman S, Guillemin K (2007) We know you are in there: Conversing with the indigenous gut microbiota. *Res Microbiol* 158:2–9.
7. Backhed F, Ley R, Sonnenburg J, Peterson D, Gordon J (2005) Host-bacterial mutualism in the human intestine. *Science* 307:1915–1920.
8. Goodrich-Blair H, Clarke D (2007) Mutualism and pathogenesis in *Xenorhabdus* and *Photorhabdus*: Two roads to the same destination. *Mol Microbiol* 64:260–268.
9. Guan C, *et al.* (2007) Signal mimics derived from a metagenomic analysis of gypsy moth gut microbiota. *Appl Environ Microbiol* 73:3669–3676.
10. Nyholm S, McFall-Ngai M (2004) The winnowing: establishing the squid-*Vibrio* symbiosis. *Nat Rev Microbiol* 2:632–642.
11. Ruby E, *et al.* (2005) Complete genome sequence of *Vibrio fischeri*: A symbiotic bacterium with pathogenic congeners. *Proc Natl Acad Sci USA* 102:3004–3009.
12. Eckburg P, *et al.* (2005) Diversity of the human intestinal microbial flora. *Science* 308:1635–1638.
13. Hooper L, *et al.* (2001) Molecular analysis of commensal host-microbial relationships in the intestine. *Science* 291:881–884.
14. Visick K, Ruby E (2006) *Vibrio fischeri* and its host: It takes two to tango. *Curr Opin Microbiol* 9:632–638.
15. Douglas A (1994) *Symbiotic Interactions* (Oxford Science Publications, Oxford, UK).
16. Dunny G, Winans S (1999) *Cell-Cell Signaling in Bacteria* (ASM Press, Washington, DC).
17. Lupp C, Ruby E (2005) *Vibrio fischeri* uses two quorum-sensing systems for the regulation of early and late colonization factors. *J Bacteriol* 187:3620–3629.
18. Visick K, Foster J, Doino J, McFall-Ngai M, Ruby E (2000) *Vibrio fischeri* lux genes play an important role in colonization and development of the host light organ. *J Bacteriol* 182:4578–4586.
19. Koropatnick T, Kimbell J, McFall-Ngai M (2007) Responses of host hemocytes during the initiation of the squid-*Vibrio* symbiosis. *Biol Bull* 212:29–39.
20. Chun C, *et al.* (2006) An annotated cDNA library of juvenile *Euprymna scolopes* with and without colonization by the symbiont *Vibrio fischeri*. *BMC Genomics* 7:154.
21. Lee M, Kim Y (2007) Signaling pathways downstream of pattern-recognition receptors and their cross talk. *Annu Rev Biochem* 76:447–480.
22. O'Grady E, Mulcahy H, Adams C, Morrissey J, O'Gara F (2007) Manipulation of host Kruppel-like factor (KLF) function by exotoxins from diverse bacterial pathogens. *Nat Rev Microbiol* 5:337–341.
23. Waxman L (1975) The structure of arthropod and mollusc hemocyanins. *J Biol Chem* 250:3796–3806.
24. Jenner R, Young R (2005) Insights into host responses against pathogens from transcriptional profiling. *Nat Rev Microbiol* 3:281–294.
25. Rodriguez-Lanetty M, Phillips W, Weis V (2006) Transcriptome analysis of a cnidarian-dinoflagellate mutualism reveals complex modulation of host gene expression. *BMC Genomics* 7:23.
26. Wilson A, *et al.* (2006) A dual-genome microarray for the pea aphid, *Acyrthosiphon pisum*, and its obligate bacterial symbiont, *Buchnera aphidicola*. *BMC Genomics* 7:50.
27. Handley S, Dube P, Miller V (2006) Histamine signaling through the H(2) receptor in the Peyer's patch is important for controlling *Yersinia enterocolitica* infection. *Proc Natl Acad Sci USA* 103:9268–9273.
28. Ruby E, McFall-Ngai M (1999) Oxygen-utilizing reactions and symbiotic colonization of the squid light organ by *Vibrio fischeri*. *Trends Microbiol* 7:414–420.
29. Antunes LC, *et al.* (2007) Transcriptome analysis of the *Vibrio fischeri* LuxR-LuxI regulon. *J Bacteriol* 189:8387–8391.
30. McFall-Ngai M (2007) Adaptive immunity: Care for the community. *Nature* 445:153.
31. Mazmanian S, Liu C, Tzianabos A, Kasper D (2005) An immunomodulatory molecule of symbiotic bacteria directs maturation of the host immune system. *Cell* 122:107–118.
32. Flentjar N, *et al.* (2007) TGF-betaRII rescues development of small intestinal epithelial cells in Elf3-deficient mice. *Gastroenterology* 132:1410–1419.
33. Ng A, *et al.* (2002) Inactivation of the transcription factor Elf3 in mice results in dysmorphogenesis and altered differentiation of intestinal epithelium. *Gastroenterology* 122:1455–1466.
34. Mysorekar IU, Lorenz RG, Gordon JI (2002) A gnotobiotic transgenic mouse model for studying interactions between small intestinal enterocytes and intraepithelial lymphocytes. *J Biol Chem* 277:37811–37819.
35. Kimbell J, Koropatnick T, McFall-Ngai M (2006) Evidence for the participation of the proteasome in symbiont-induced tissue morphogenesis. *Biol Bull* 211:1–6.
36. Kimbell J, McFall-Ngai M (2004) Symbiont-induced changes in host actin during the onset of a beneficial animal-bacterial association. *Appl Environ Microbiol* 70:1434–1441.

Supporting Information

Chun *et al*. 10.1073/pnas.0802369105

SI Text

Squid Colonization Experiments. The breeding stock of adult *Euprymna scolopes* was maintained and bred under laboratory conditions as previously described (1). Because the juveniles used in this study were the progeny of a number of field-caught animals, and were hatched over the course of two weeks, we sought to minimize the effects of natural genetic variation. To achieve this aim, the animals that hatched on a given day were equally divided among the six treatments. As a result of this strategy, the pooled RNA from a given treatment was derived from six to eight separate clutches, laid by three to four different field-caught females.

Four biological replicates (i.e., separate light-organ RNA extractions of independently collected light organs, each containing 90 organs for each of the six colonization treatments) were performed on the same day with the same reagents. Thus, a total of 540 organs were sampled for each of the four biological replicates.

The newly hatched juvenile animals were colonized by exposure to either wild-type, *luxA* or *luxI* strains of *Vibrio fischeri*. The *luxA* mutant has a deletion in a gene encoding bacterial luciferase, and is completely defective in bioluminescence, while the *luxI* mutant is unable to synthesize 3-oxo-hexanoyl-L-homoserine lactone (AI), an autoinducer of luciferase. The *luxI* mutant makes only a reduced level of luminescence (2). Because AI spontaneously inactivates in the alkaline conditions of seawater (3), we determined the rate of loss under our experimental conditions (Fig. S2). The resulting data indicated that by supplementing the seawater with 6 μM AI, the concentration of this luminescence inducer remained above 100 nM, the approximate level found in light organs colonized by wild-type cells (4), throughout the incubation (i.e., from 6 to18 h post inoculation). The efficacy of this AI-addition protocol was additionally confirmed by the restoration of the luminescence of animals colonized by the *luxI* mutant to a level close to that characteristic of colonization by wild-type *V. fischeri* (Fig. S3).

Microarray Hybridizations. The spotted microarray contained 13,962 cDNAs (5) applied two times on each glass slide, for a total of 27,924 sample spots (GEO accession: Platform GLP3825; I. V. Koroleva, B. J. Brown, E. Snir, H. Almabrazi, T. L. Casavant, M. B. Soares, and M. McFall-Ngai; Squid EST 30K cDNA array; public on June 2, 2006). The microarray slides had five positive-control spikes prepared using sequences isolated from *Xenopus leavis*, *Anopheles gambiae, Schistosoma mansoni*, and *Apis mellifera* (6–8). The chosen sequences did not cross-hybridize with any of the cDNAs from the *E. scolopes* light organ EST database (data not shown). Negative controls were spots of (*i*) buffer alone, (*ii*) polyA oligonucleotides, or (*iii*) no template.

Pools of light organs, obtained from 90 juvenile squid subjected to the same treatment, were homogenized (Polytron 1200C, Brinkmann Instruments Inc.), and total RNA was extracted using the MasterPure Purification Kit (Epicentre Biotechnologies), followed by the RNeasy Mini Kit with on-column DNase digestion (Qiagen Inc.). The resulting RNA sample was concentrated with a Microcon 30 (Millipore). The concentration and quality of the samples were determined spectrophotometrically, and their purity was estimated by agarose gel electrophoresis. Each biological replicate of 90 light organs contained on average 20 μg of total RNA, and only samples with a 260/280 nm optical ratio of between 1.9 and 2.0 were used. Visual inspection revealed two distinct ribosomal bands and no evidence of degradation products (data not shown). Total RNA samples were processed and indirectly labeled with 3DNA 350HS Expression Array Detection Kit (Genisphere). Slides were hybridized overnight, and washed using a Lucidia SlidePro hybridization station (GE Healthcare). The arrays were then scanned using GenePix 4000B (Molecular Devices). The raw data were stored in the database, and used for subsequent analysis.

On each slide we used a runoff reference, which is a mixture of vector-primed transcription products derived from an equal mixture of the 13,962 *E. scolopes* cDNA clones, labeled with the same protocol as the experimental samples (see below). This approach allowed us to compare each experimental condition to a single standardized reference, and to use a robust normalization method, the two-way semilinear model (TW-SLM) (9), that has been specifically optimized to identify genes in our experimental design. Each spotted glass-slide microarray was hybridized with two samples: (*i*) the experimental cDNA; and, (*ii*) the run-off reference, using a procedure described previously (10) except that sheared *E. scolopes* genomic DNA was used to block repetitive elements. This genomic DNA was isolated from a freshly dissected adult squid using the Blood and Cell Culture DNA Maxi Kit (Qiagen Inc.). As a control for technical variation inherent in the fluorescent-probe chemistry, the Cy3 and Cy5 labeling of the experimental sample and the run-off reference were alternated in at least two slides per replicate (i.e., three replicates per condition) in each of the six conditions. After normalization of the arrays' hybridization signals, Volcano plot analyses and ANOVA (see below) were performed on data from the six treatment conditions. These analyses identified 781 RNA transcripts/genes that were significantly differentially regulated between the conditions (Table S4).

Microarray Significance Analysis. To determine the confidence level of the signals from the hybridized glass-slide microarrays, we first accounted for the dye-swap technical replication, followed by a further independent normalization using two different techniques: per spot per chip (PSPC) and two-way semilinear model (TW-SLM) (9). All statistics described below were performed using GeneSpring GX software (Agilent Technologies). To eliminate systematic error due to either inconsistency of replicates or intensity levels below a reliable range, both raw and control data were filtered with 50% confidence according to the cross-gene error model for normalization conditions, both with and without the consideration of spike controls (11). The resulting 7,503 transcripts were analyzed using two statistical methods: (*i*) Volcano plot analysis with a fold-change threshold of 2.0 and a P value ≤ 0.05; and (*ii*) analysis of variance (ANOVA) with a P value ≤ 0.05, using Benjamini and Hochberg false discovery rate (FDR) multiple-testing correction (12) followed by Tukey's pair-wise comparison (Table S1).

To assess whether the hybridization signals that had been detected were specific to cDNA spots, we compared the mean spot intensity (meanS) with the mean of the median local background intensity (meanB) for each slide. Each spot was given a reliability score ranging from 0 to 4 (0 = meanS $\leq$ meanB; one point is given for each standard deviation (SD) greater than the background, and 4 = meanS > meanB + 3SD). Scores for all replicates were averaged. Spots with scores of 3 and 4 are considered highly reliable. Of the 13,962 sequences tested on the microarray, 12,616 sequences (90.4%) had an average score of 4 and 1130 sequences (8.1%) had an average score of

3 (Table S4). Approximately, 98% (765 of 781) transcripts found to be significantly differentially regulated in at least one pairwise comparison of the microarray analyses had an average reliability score of 3 or 4.

Quantitative AI Assay. To determine the amount of biologically active AI predicted to be remaining in HOSW (pH 8.2 at 23°C) throughout the 18-h incubation of animals to be used in the microarray experiment, we used a quantitative bioassay with *Escherichia coli* (pHV200I$^-$) as described (3). Levels of AI were monitored over a 12 h period in either the presence or absence of uncolonized juvenile squid. Synthetic AI (Sigma-Aldrich) was resuspended as a solution and stored in acidified ethyl acetate (EtAc). Immediately before use, the AI solution was dispensed to a glass vial, dried under nitrogen gas and dissolved in 2 ml of HOSW to a final concentration of 6 μM. The pH and temperature of the water was measured at the start and end of each experiment. At the onset and at various times throughout the experiment, 6 μl of the HOSW containing AI were removed from the sample and added to 100 μl of EtAc. These samples were stored in airtight glass vials at -20°C before bioassay (3).

Bioluminescence Colonization Assay. The minimum concentration of exogenously added AI necessary to complement the luminescence of the *V. fischeri luxI* mutant to wild-type levels was determined as follows. Sets of 12 newly hatched squids were placed in HOSW inoculated with either the wild type or the *luxI* mutant strain of *V. fischeri*. After 6 h, the animals were transferred to fresh HOSW containing different concentrations of AI, and the level of squid bioluminescence that subsequently developed was monitored for 28 h (Fig. S3) using an automated photometer (13). Data presented are representative of two independent trials, and indicated that AI added to a concentration of 200 nM would induce and maintain the luminescence of the *luxI* mutant at nearly wild-type levels for at least 12 additional hours.

Quantitative Real-Time PCR. To verify the differential expression of a subset of genes identified in the microarray analyses, QRT-PCR was performed on selected transcripts (Table S3). To ensure that differential gene regulation identified in the microarray consistently occurs (i.e., irrespective of the cohort of animals or the reagent lot), the RNA for QRT-PCR analysis was derived from light organs that had been isolated from a fourth cohort of animals at the same time as the three sets of samples collected for the microarrays. Actin-specific primers were used as a control (Table S3) because previous work (14), as well as this study (data not shown), indicated that the levels of actin transcript do not change during the first few days of light-organ development. Standard curves were created using a 10-fold cDNA dilution series with each primer set. The Pfaffl method (15) was used to calculate the fold-change in transcript abundance between each condition. The efficiencies of all QRT-PCR reactions were between 90% and 105%, although the range between any two reactions used to determine fold-change was <10%. All reactions used to determine fold-change were constructed from the same set of cDNA dilutions.

QRT-PCR was performed using iQSYBR Green Supermix in an iCycler Thermal Cycler (Bio-Rad Laboratories). Gene-specific primers were designed to create a product between 83 and 148 bp (Table S3), and amplification was performed under the following conditions: 95°C for 5 min, followed by 50 cycles of 95°C for 15 sec, a specific annealing temperature (Table S3) for 15 sec, and 72°C for 15 sec. Each reaction was performed in triplicate and contained 0.2 μM primers and 3.0 mM $MgCl_2$. To determine whether a single amplicon resulted from this PCR, the presence of only one optimal dissociation temperature was assayed by incrementally increasing the temperature every 10 sec from 60 to 89.5°C.

Antibody Production and Immunocytochemistry with Antibodies to EsLBP. For the production of an antibody to EsLBP, we analyzed the derived amino acid sequence of the open-reading frame of the transcript to identify a peptide region of high antigenicity, surface probably, and hydrophilicity. The resulting candidate, a 20 amino acid peptide (DNKTDCNGEQDGRHECENSQ), was conjugated to bovine gamma globulin and injected intramuscularly into chickens for production of polyclonal hen-egg antibodies. In addition, before injection with the antigen, eggs were collected for the preimmune controls. Antibodies were concentrated by polyethylene-glycol precipitation from both the eggs of preimmunized and immunized hens. The EsLBP antibody was characterized by western-blot analysis, which showed that the antibody recognizes a single peptide at the molecular mass predicted for the derived amino acid sequence corresponding to the gene encoding the protein.

Immunocytochemistry (ICC) was performed as described (14). Briefly, juvenile squid were anesthetized in 2% ethanol in seawater, and fixed overnight at 4°C in 4% paraformaldehyde in marine PBS (mPBS) consisting of 50 mM sodium phosphate buffer with 0.45 M NaCl, pH 7.4. Animals were then rinsed 4 times for 30 min in mPBS. The samples were then permeabolized for 2 days at 4°C in 1 ml of 1% Triton X-100 in mPBS with mixing. They were then blocked overnight at 4°C in a solution of 1% Triton X-100, 2% goat serum, and 0.5% BSA in mPBS. The samples were incubated with 1:1000 dilution of the anti-EsLBP polyclonal antibody in blocking solution for two weeks at 4°C. Samples were then rinsed 4 times for 1 h in 1% Triton X-100 in mPBS, and incubated overnight in blocking solution at 4°C. Fluorescein isothiocyanate (FITC)-conjugated to goat anti-chicken secondary antibody (Jackson Immunoresearch) was added at a 1:250 dilution to fresh blocking solution containing a1:2500 dilution of a rhodamine phalloidin counterstain, which labels filamentous actin, and the samples were incubated in the dark overnight at 4°C. Samples were rinsed 4 times at 30 min in 1% Triton X-100 in mPBS, followed by two final rinses in mPBS. The tissues were then counterstained with the nucleic acid TOTO-3 (Invitrogen, Inc.) following the manufacturer's instructions. Samples were then mounted on glass slides in Vectashield (Vector Laboratories), a mounting medium that retards photobleaching. Preimmune chicken antibodies (at a dilution of 1:1,000) were used as a control for non-specific binding of chicken antibodies to host tissues. To determine whether the EsLBP antibody adheres non-specifically to bacteria, we treated culture-grown cells of *V. fischeri* to the above protocol with both preimmune and immune hen-egg antibodies. The cells were then counterstained with 500 nM propidium iodide. All confocal experiments were performed on a Zeiss LSM 510 system.

Statistical Treatment of Comparisons with Mouse and Zebrafish Microarray Data. To determine whether there was a significance to the overlap between symbiosis-induced genes in the vertebrate and the squid expression studies, we calculated the probability that the 16-gene overlap in these studies could have occurred by chance. Specifically, the question was: Given that 462 of the 7503 expressed squid genes vary significantly between the symbiotic and the aposymbiotic conditions, what is the likelihood of observing 16 symbiosis-expressed squid genes among the 45 total genes shared between the squid library and the subset of vertebrate genes that are differentially expressed by interaction with the normal microbiota? To determine this likelihood, we applied both the Fisher's Exact test and the χ^2 test; because one specific gene set was analyzed, a correction for multiple testing was not needed. The finding that 16 of 45 genes are shared in the two comparisons showed high levels of significance by both analyses (Fisher's Exact test, $P = 3.3 \times 10^{-7}$; χ^2, $P = 1.2 \times 10^{-10}$).

1. Doino J, McFall-Ngai M (1995) Transient exposure to competent bacteria initiates symbiosis-specific squid light organ morphogenesis. *Biol Bull* 189:347–355.
2. Visick K, Foster J, Doino J, McFall-Ngai M, Ruby E (2000) *Vibrio fischeri* lux genes play an important role in colonization and development of the host light organ. *J Bacteriol* 182:4578–4586.
3. Schaefer AL (2000) Detection, purification, and structural elucidation of the acylhomoserine lactone inducer of *Vibrio fischeri* and other related molecules. *Methods Enzymol* 305:288–301.
4. Boettcher KJ, Ruby EG (1995) Detection and quantification of *Vibrio fischeri* autoinducer from symbiotic squid light organs. *J Bacteriol* 177:1053–1058.
5. Chun, C, *et al.* (2006) An annotated cDNA library of juvenile *Euprymna scolopes* with and without colonization by the symbiont *Vibrio fischeri. BMC Genomics* 7:154.
5. Blackshear PJ, *et al.* (2001) The NIEHS *Xenopus* maternal EST project: interim analysis of the first 13,879 ESTs from unfertilized eggs. *Gene* 267:71–87.
6. Franco GR, *et al*. (1995) Identification of new *Schistosoma mansoni* genes by the EST strategy using a directional cDNA library. *Gene* 152:141–147.
7. Nunes FM, *et al.* (2004) The use of Open Reading frame ESTs (ORESTES) for analysis of the honey bee transcriptome. *BMC Genomics* 5:84.
8. Wang D, Huang J, Xie H, Manzella L, Soares MB (2005) A robust two-way semi-linear model for normalization of cDNA microarray data. *BMC Bioinformatics* 6:14.
9. Whitfield CW, *et al.* (2002) Annotated expressed sequence tags and cDNA microarrays for studies of brain and behavior in the honey bee. *Genome Res* 12:555–566.
10. Peng X, *et al*. (2003) Statistical implications of pooling RNA samples for microarray experiments. *BMC Bioinformatics* 4:26.
11. Benjamini Y, Drai D, Elmer G, Kafkafi N, Golani I (2001) Controlling the false discovery rate in behavior genetics research. *Behav Brain Res* 125:279–284.
12. Millikan DS, Ruby EG (2004) Vibrio fischeri flagellin A is essential for normal motility and for symbiotic competence during initial squid light organ colonization. *J Bacteriol* 186:4315–4325.
13. Kimbell J, McFall-Ngai M (2004) Symbiont-induced changes in host actin during the onset of a beneficial animal-bacterial association. *Appl Environ Microbiol* 70:1434–1441.
14. Pfaffl M (2001) A new mathematical model for relative quantification in real-time RTPCR. *Nucleic Acids Res* 29:e45.
15. Handley S, Dube P, Miller V (2006) Histamine signaling through the H(2) receptor in the Peyer's patch is important for controlling *Yersinia enterocolitica* infection. *Proc Natl Acad Sci USA* 103:9268–9273.

A

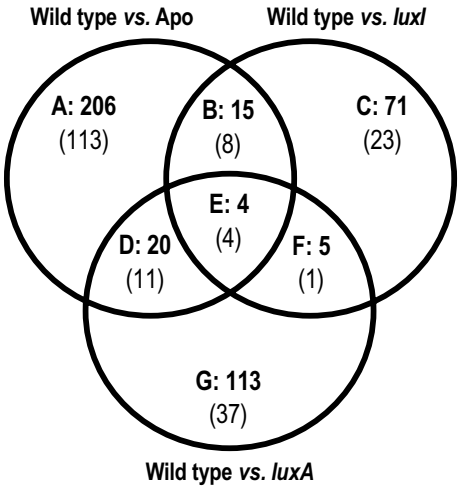

Number of light-organ transcripts regulated in response to:

A – the presence of symbionts, regardless of light or AI
B – AI, regardless of symbionts
C – AI, in the presence of symbionts
D – light, regardless of symbionts
E – AI or light, regardless of symbionts
F – AI or light, in the presence of symbionts
G – light, in the presence of symbionts

B

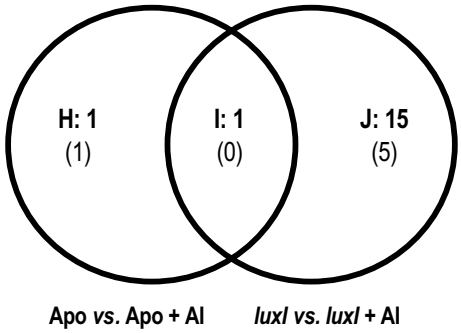

H -- added AI, in the absence of *luxI* symbionts
I -- added AI, regardless of light or *luxI* symbionts
J -- added AI, in the presence of *luxI* symbionts

C

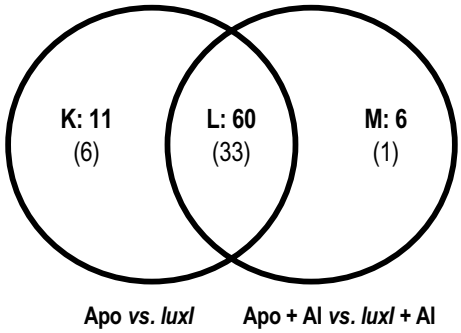

K -- the presence of *luxI* symbionts, in the absence of AI
L -- the presence of *luxI* symbionts, regardless of AI
M -- the presence of *luxI* symbionts, in the presence of added AI

Fig. S1. Venn diagrams summarizing transcriptional responses of the light organ to (*A*) colonization by symbionts that either do or do not produce light or AI, and (*B* and *C*) colonization by the *luxI* mutant in the presence or absence of added AI. The responses defined by each quadrant (expression classes A-M) are listed. The numbers of total transcripts, as well as those with known annotations (in parentheses), that are differentially regulated ≥2 fold in all of the relevant comparisons are given.

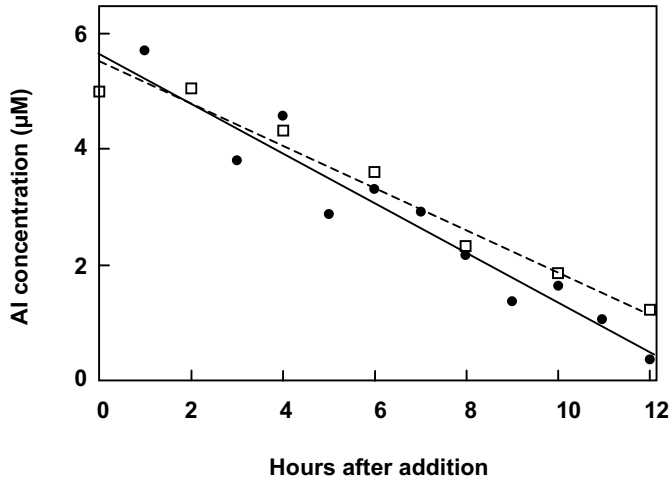

Fig. S2. Rate of spontaneous degradation of AI in seawater. AI concentration, as determined by bioassay (see *SI Text*) decreased linearly when synthetic AI (6 μM) was added to HOSW. Data are means of triplicate samples from three independent trials. Similar results were found when aposymbiotic squid were either absent (closed circles) or present (open squares) in the HOSW. Rates of degradation, calculated for these two conditions by linear regression, are indicated by the solid and dotted lines, respectively.

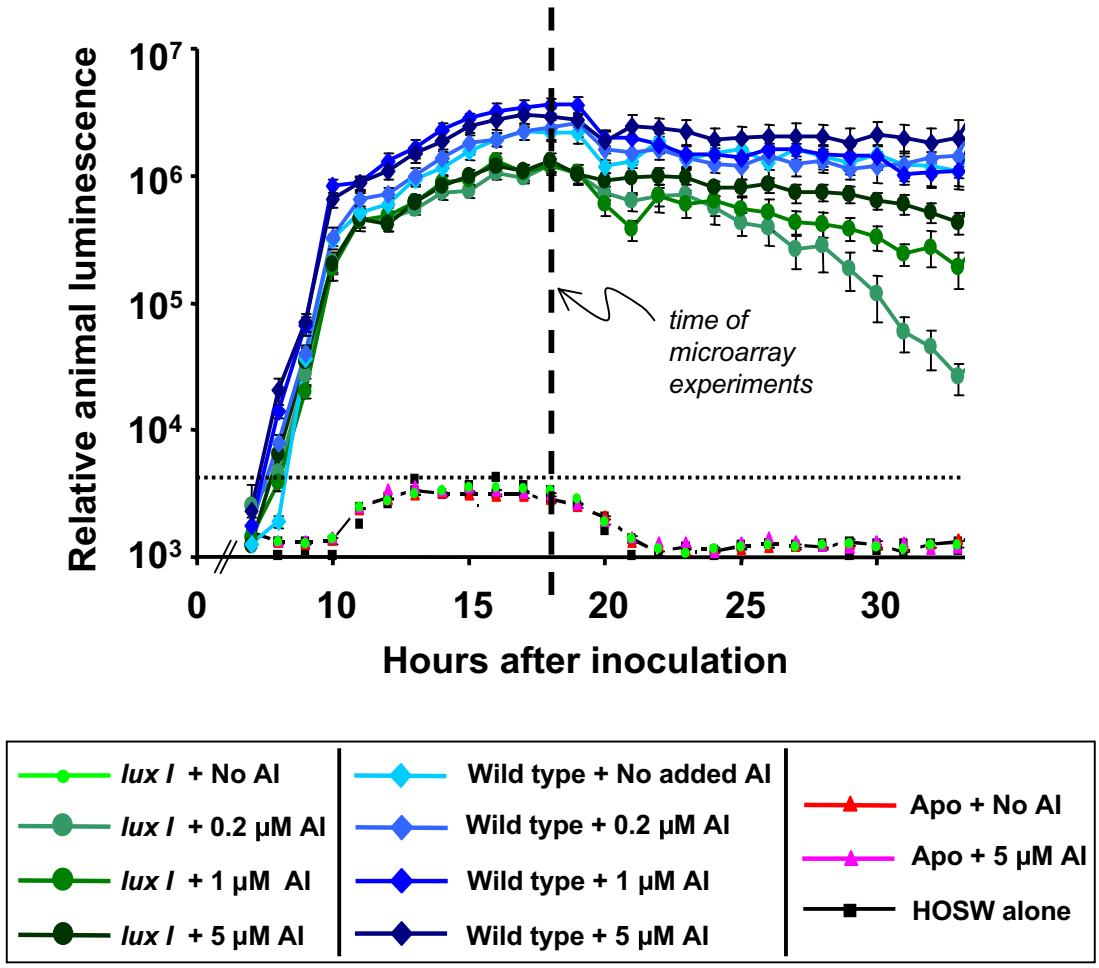

Fig. S3. Complementation of the symbiotic luminescence of a *V. fischeri luxI* mutant by the addition of synthetic AI. Sets of 12 newly hatched juvenile squid were placed in HOSW inoculated with either *V. fischeri* wild type (diamonds) or a *luxI* mutant strain (circles). After 6 h, the animals were transferred to uninoculated HOSW to which different concentrations of synthetic AI were added, and the development of symbiotic luminescence was followed. The luminescence level was determined every hour and averaged over the sets. Data shown represent the results of one of two independent trials, both of which showed the same trend. The time (18 h postinoculation) at which animals were sampled for the microarray experiments (see *SI Text*) is indicated by the vertical dashed line. Luminescence of aposymbiotic (uninoculated) animals, and animals inoculated with the *luxI* mutant in the absence of added AI, remained below the maximum level of background light (dotted line). The small increase in background luminescence observed between 10 and 22 h was due to an instrumental light leak during the daily 12-h period that the room lights were on (the animal's ''day''). More sensitive measurements indicated that the *luxI* mutant (without AI) produced bioluminescence at ≈0.1% of wild-type levels (ref. 2 and data not shown).

Table S1. Summary of ranges for light-organ transcript differentially regulated under different conditions

Comparisons*	Total number of transcripts†	Range of fold-changes of differentially regulated transcripts‡			Expression class§
		Known	Unknown/Hypo	No hits	
Category conditions					
Symbiont vs. no symbiont	132	8.6 – (−3.7)	9.4 – (−3.4)	2.8 – (−5.0)	N
Light vs. no light	27	4.7 – (−1.8)	4.9 – (−2.3)	2.3 – (−2.5)	P
AI vs. no AI	10	3.4 – 1.5	2.6 – 1.5	n.a.¶	O
Individual conditions					
Wild type vs. apo	462	130 – (−20)	29 – (−13)	100 – (−10)	A, B, D, E
Wild type vs. *luxA*	211	69 – (−48)	64 – (−27)	100 – (−10)	D, E, F, G
Wild type vs. *luxI*	131	21 – (−25)	54 – (−180)	8.9 – (−37)	B, C, E, F
Wild type vs. *luxI* + AI	24	11 – (−7.1)	12 – (−50)	4.2 – (−2.3)	Q
Apo vs. apo + AI	13	2.4	27	n.a.	H
Apo vs. *luxI*	154	3.5 – (−33)	4.3 – (−25)	3.6 – (−20)	K, L
Apo + AI vs. *luxI* + AI	148	4.5 – (−10)	3.3 – (−4.8)	20 – (−3.1)	L, M
luxI vs. *luxI* + AI	32	3.4 – (−11)	26 – (−8.3)	24 – (−9.1)	I, J

*Differences between conditions sharing the same category of exposure condition. ''Symbiont'' includes wild type, *luxI*, *luxI* + AI, and *luxA*; ''no symbiont'' includes apo and apo + AI; ''light'' includes wild type and *luxI* + AI; ''no light'' includes apo, apo + AI, and *luxA*; ''AI'' includes wild type, *luxA, luxI* + AI, and apo + AI; and ''no AI'' includes apo and *luxI.*

†Number of transcripts differentially regulated between conditions (see *Methods*).

‡Known, related to a described gene; unknown/hypo, undescribed or hypothetical protein; no hits, no significant homology to the nonredundant database of Genbank as determined by BLASTX analysis.

§Letter designation indicates the expression class in Fig. S1 and/or Table S4.

¶n.a., not applicable.

Table S2. Transcripts regulated in grouped conditions (the presence of symbionts, luminescence and/or AI)

Identifier	Annotation of transcript*	Fold change† S/NS	L/NL	A/NA‡
Require symbionts producing luminescence and AI§ (*n* = 8)				
SQabh-m-16	Lipopolysaccharide binding protein (LBP/BPI)	8.6	4.4	3.4
SQaaf-h-03	Peptidoglycan recognition protein 1 (PGRP1)	7.3	4.7	2.2
SQaab-n-03	Galaxin-1 (invertebrate protein; unknown function)	4.8	3.3	2.6
SQabd-a-21	Galaxin-2 (invertebrate protein; unknown function)	4.1	2.9	2.2
SQaay-n-03	Tetraspanin 3 (TSPAN3) regulator of membrane protein trafficking	2.2	1.9	1.5
SQaaq-p-05	Unknown	9.4	4.9	2.6
SQabd-h-03	Unknown	4.1	3.5	1.9
SQaaw-d-09	Hypothetical	2.8	2.4	1.5
Require symbionts producing luminescence (no AI)				
SQaab-c-08	Rhomboid domain-containing 1 (RHBDD1) membrane protease	3.4	2.7	
SQaao-n-19	Glutamate receptor, ionotropic, N-methyl D-aspartate-assoc. 1 (GRINA)	2.2	2.4	
SQaae-d-01	M2 (small) subunit of ribonucleotide reductase (RRM2) (DNA synthesis)	2.0	2.5	
SQaal-j-05	Guanylate cyclase 1, soluble, beta 2 (GUCY1B2), retina-associated	−2.4	−1.8	
SQaap-o-17	Unknown	2.7	2.1	
SQabc-k-15	No significant hits	2.5	2.0	
SQaaa-g-18	Hypothetical	−2.4	−2.1	
SQabf-h-04	Unknown	−2.7	−2.3	
SQaaf-i-15	No significant hits	−3.2	−2.5	
Require symbionts producing AI (no luminescence) *(n = 2)*				
SQabb-g-13	CCAAT enhancer binding protein (CEBPB)	2.4		1.7
SQaac-i-20	DC12 (unknown function)	2.3		1.7
Require symbionts (no luminescence, no AI) *(n = 51)*				
SQabe-n-18	ETS-family transcription factor (ELF3)	3.3		
SQaao-p-19	Fas apoptotic inhibitory molecule 2 (FAIM2)	3.2		
SQaaj-n-15	Calsequestrin 1 (CASQ1) calcium-binding protein	2.9		
SQaak-m-10	Transposase	2.6		
SQaac-f-23	Vertebrate adenosine A3 receptor (ADORA3)	2.4		
SQaba-a-08	Cullin-3 (CUL-3) (proteasome/ubiquitin pathway of protein degradation)	2.3		
SQabi-l-15	Integrin, beta 1 (ITGB1) extracellular-matrix protein	2.3		
SQaaa-n-06	Solute carrier family 1 (GLAST), glutamate transporter	2.3		
SQaar-j-17	Super cysteine-rich protein (SCRP)	2.2		
SQabd-d-05	Low-density lipoprotein receptor-rel. prot. 2 (Megalin, gp330) (endocytosis)	2.2		
SQaaq-f-07	Peptidoglycan recognition protein 2 (PGRP2)	2.0		
SQaaw-l-02	Annexin A7 (Synexin) calcium-binding protein	2.0		
SQaai-b-17	Receptor (TNFRSF)-interacting serine-threonine kinase 1	−2.0		
SQabf-n-17	Dynein heavy chain 7 (DHC7), cilia associated	−2.0		
SQaas-p-14	Testis specific gene A2 (TSGA2) (assoc. with motility, and egg interaction)	−2.0		
SQaab-b-03	TBC (Tre-2/Bub2/Cdc16) domain (GTPase activation)	−2.0		
SQaag-l-03	AKAP-associated sperm protein (ASP) (phosphorylation; sperm motility)	−2.0		
SQaaz-m-12	Doublecortin and CaM kinase-like 3 (DCAMKL3), microtubule-associated	−2.0		
SQabk-g-07	Golgi autoantigen, golgin subfamily a, 4 (membrane trafficking)	−2.1		
SQabc-h-02	Uroporphyrin-III C-methyltransferase (regulation of porphyrin synthesis)	−2.1		
SQaau-o-20	Stromal protein associated with thymus and lymph nodes isoform 2	−2.1		
SQaab-j-01	Zonadhesin isoform 2 (ZAN), sperm protein associated with binding to egg	−2.1		
SQabe-l-09	Mitogen-act. prot. kinase kinase kinase 9 (MAP3K9) (c-Jun/JNK apoptosis)	−2.2		
SQabk-o-09	Sperm-tail protein SHIPPO1 isoform 2 (ODF3)	−2.2		
SQaat-f-20	Reticulocyte binding protein 2b	−2.3		
SQabb-h-05	Lamin (LAM) nuclear-associated intermediate filament	−2.3		
SQaae-h-11	Excision repair complementing rodent repair deficiency, comp. (ERCC8)	−2.4		
SQaaw-l-14	Annexin A7 (Synexin) calcium binding protein	−2.6		
SQabc-e-07	Ciliary rootlet coiled-coil, rootletin protein	−2.6		
SQaae-j-15	Axonemal dynein heavy chain 7 (DNAHC7) sperm/ciliary microtubule prot.	−2.7		
SQaac-h-19	Dual-specificity tyrosine-(Y)-phosphorylation reg. kinase4 (DYRK4) (testes)	−3.7		
SQaaw-i-02	No significant hits	2.8		
SQaaq-c-05	No significant hits	2.8		
SQabj-d-01	Unknown	2.7		
SQaaq-d-04	No significant hits	2.6		
SQaam-h-22	Hypothetical	2.2		
SQaap-m-24	No significant hits	2.0		
SQaaf-h-16	Unknown	−2.0		
SQaaa-f-22	No significant hits	−2.0		
SQaaw-d-08	No significant hits	−2.1		

Identifier	Annotation of transcript*	Fold change†		
		S/NS	L/NL	A/NA‡
SQaar-l-19	Unknown	−2.1		
SQaax-c-19	Hypothetical	−2.1		
SQaaj-e-07	Unknown	−2.3		
SQaar-n-21	No significant hits	−2.3		
SQaac-h-09	Hypothetical	−2.3		
SQaat-b-08	Hypothetical	−2.3		
SQaao-l-06	No significant hits	−2.5		
SQabc-l-03	Hypothetical	−2.6		
SQaad-j-22	No significant hits	−2.8		
SQaab-e-07	Hypothetical	−3.4		
SQaag-n-09	No significant hits	−5.0		
Require luminescence only *(n = 2)*				
SQabf-o-02	No significant hits	2.3		
SQabh-m-05	Unknown	2.1		
Total number of transcripts in each category:		70	19	10

*Classified based on whether their responses required one, two, or all three of the conditions; no transcripts were found that responded either solely to the presence of AI, or to light and AI.

†Those transcripts up- or down-regulated ≥2-fold in all four normalizations, calculated as the first condition relative to the second; S/NS, symbionts vs. no symbionts; L/NL, light vs. no light; or A/NA, AI vs. no AI.

‡Transcripts in the A/NA category were not always significantly differentially regulated in all four normalizations.

§Category of grouped conditions; *n* = total number of transcripts.

Table S3. QRT-PCR confirmation of microarray transcript regulation

Gene	Fold change		Primer sequences	Annealing temperature/product size*
	Microarray	QRT-PCR		
WT vs. Apo†				
Transcription factor IIB (TFIIB)	−1.9	−1.8	Forward: 5′AAT GCC GAT GCG TCT TGA TGA TGG Reverse: 5′ AAT TGC TGC CAT AAG CTC TGC GTG	58°C/83 bp
NADPH oxidase (gp91phox) (CYBB)	−1.8	−2.0	Forward: 5′GCC AAC ACC TGA CCA ACT TCC AAT Reverse: 5′TTC CCG TGC CGA TAA ATA CGT CCA	58°C /104 bp
Matrix metalloproteinase 17 Preproprotein (MMP17)	3.2	2.7	Forward: 5′GCC AGA TTG GTT GGC TTT CCT CTG Reverse: 5′GAC GCA GCC ATT TCG TCC GAT AAC	61°C /113 bp
Low density lipoprotein receptor-related protein 2 (Megalin, gp330)	4.3	4.0	Forward: 5′TTC AAT GCG CGC ACT AAT TGG AGG Reverse: 5′ACT TAG CCG CCA CTA TGA AGC TGA	58°C /122 bp
M2 (small) subunit of ribonucleotide reductase (RRM2)	2.8	2.6	Forward: 5′AGA ATT GTC GCC TTT GCT GCT GTG Reverse: 5′CCG GCA TCA CAG AGC GTT TCT TTA	58°C / 91 bp
LBP	11.5	10.5	Forward: 5′CTG ACT GCA ATG GAG AGC AAG ACG Reverse: 5′ CAC TGA CTG CCT TAC ACT GGC AAC	62°C / 84 bp
Glutathione peroxidase	−1.9	−1.7	Forward: 5′CCA GAT GAA TGA GCT GGT CG Reverse: 5′CCA GGA CGG ACA TAG CAA AG	61°C /132 bp
WT vs. *luxA*†				
Hemocyanin	68.9	8.7	Forward: 5′CAG TAG TCG GTC TGT TCC AAG GCT Reverse: 5′TTA GTC CAG AGA CGA TGA CCG CAC	62°C /122 bp
MMP19	−2.3	2.3	Forward: 5′ TCC ACC GAC TAC AAC CAC GAA CAA Reverse: 5′ CCT TTG CAT CTG TGA AGG CTG CTT	62°C / 92 bp
Colony stimulating factor	15.4	5.0	Forward: 5′TCG CCC GTG GAA ATT ACG ATC CTG Reverse: 5′GAT GGC GCG TGT TTG TTC AGC TTC	61°C /103 bp
Control transcript	not	not	Forward: 5′GAG CGT AAA TAC TCT GTC	
Actin	regulated	regulated	Reverse: 5′GAG AAT TTG TAG AGT AGC G	56°C /148 bp

*Annealing temperature at which efficiencies were between 90 and 105%.
†Conditions being compared.

Table S6. Symbiosis-regulated genes shared among different hosts

Regulated in zebrafish and mouse, but not in *E. scolopes*

1. angiogenin 4
2. C-reactive protein, pentraxin-related
3. deleted in malignant brain tumors 1; crp-ductin
4. deoxythymidylate kinase (thymidylate kinase)
5. farnesyl diphosphate synthetase
6. fat specific gene 27
7. RNA-binding protein FUS
8. glial cell line derived neurotrophic factor family receptor alpha 1
9. interferon-related developmental regulator 1
10. immunoresponsive gene 1
11. peroxisome proliferative activated receptor, alpha
12. scinderin
13. serum/glucocorticoid regulated kinase
14. transferrin receptor

Regulated in zebrafish and mouse; present in *E. scolopes,* but not regulated

1. angiotensin converting enzyme
2. apolipoprotein B
3. arginase 2
4. ATP-binding cassette, sub-family C (CFTR/MRP), member 2
5. B-cell leukemia/lymphoma 6
6. complement component 3
7. cytochrome P450, family 7, subfamily A, polypeptide 1
8. exostoses (multiple) 1
9. fasting-induced adipose factor; angiopoietin-like 4
10. FK506 binding protein 5
11. flap structure specific endonuclease 1
12. four and a half LIM domains 1
13. fructose-1,6-bisphosphatase 1
14. growth arrest and DNA-damage-inducible, beta
15. H2A histone family, member X
16. heterogeneous nuclear ribonucleoproteins methyltransferase-like 2 (S. cerevisiae)
17. interferon-induced protein with tetratricopeptide repeats 1
18. lactate dehydrogenase B
19. lectin, galactoside-binding, soluble, 9 (galectin 9)
20. nuclear receptor subfamily 1, group D, member 2; Rev-ErbA-beta
21. peptidylprolyl isomerase C-associated protein
22. phenylalanine hydroxylase
23. phosphatidylinositol 3-kinase, regulatory subunit, polypeptide 1 (p85 alpha)
24. serum amyloid A1
25. suppressor of cytokine signaling 3
26. tropomyosin 3, gamma
27. tryptophanyl-tRNA synthetase
28. tyrosyl-tRNA synthetase
29. VAMP (vesicle-associated membrane protein)-associated protein A, 33kDa

Regulated in zebrafish and mouse; present in *E. scolopes,* and symbiont-regulated

1. proteasome (prosome, macropain) subunit, alpha type 5
2. ADP-ribosylation factor 1
3. tumor necrosis factor, alpha-induced protein 2
4. E74-like factor 3 (ETS domain transcription factor, ELF3, epithelial-specific)
5. ribonucleotide reductase M2
6. solute carrier family 31 (copper transporters), member 1
7. arginine-rich, mutated in early stage tumors
8. phosphogluconate dehydrogenase
9. hydroxysteroid (17-beta) dehydrogenase 2
10. cathepsin L
11. N-sulfotransferase
12. solute carrier family 34 (sodium phosphate), member 2
13. calcium binding protein 5 (centrin)
14. glutathione peroxidase 2 (gastrointestinal)
15. cysteine rich protein 2
16. vacuolar protein sorting 35

Vertebrate–species annotation shown.

Table S7. Squid, zebrafish, and mouse transcripts differentially regulated in response to symbiont colonization

Transcript annotation	Predicted function	Fold change*		
		Squid	Zebrafish	Mouse
Proteasome (prosome, macropain) α 1 (PMSA1)†	NF-kappaB pathway	130	2.5	2.8
ADP-ribosylating factor 6 interacting protein (ARL6AIP)†‡	Cell cycle arrest and apoptosis	97	2.6	2.0
Tumor necrosis factor, alpha-induced protein (TNFAIP8)†‡	NF-kappaB pathway	12	2.3	5.6
ETS-family transcription factor (ELF3)‡§	Epithelial differentiation, apoptosis, iNOS	4.6	−5.3	2.6
Ribonucleotide reductase M2 (RRM2)§	Cellular proliferation, induces NF-kappaB activity	2.8	3.1	2.3
Solute carrier family (SLC1)†‡	Enhanced cellular uptake of long-chain fatty acids	2.0	−2.5	−4.0
Arginine-rich mutated in early stage tumors (ARMET)§	Unknown	1.7	3.8	2.5
Phosphogluconate dehydrogenase§	Pentose phosphate shunt/reactive oxygen species	1.7	2.3	2.6
Hydroxysteroid (17-beta) dehydrogenase 12b†‡	Metabolism	1.6	−2.3	−2.5
Cathepsin L (CTSL)‡§	Acid-dependent lysosomal cysteine protease	1.5	2.3	2.8
Sulfotransferase‡§	Development, immune response	−1.7	2.0	−2.5
Centrin†‡	Cell division	−1.8	2.8	3.0
Glutathione peroxidase (GPX)†	Oxidative burst pathway	−1.9	2.7	1.9
Ataxin (super cysteine-rich protein 2) (SCRP)†‡	Stress granule and P-body assembly, apoptosis	−1.9	3.2	3.2
Solute carrier family (SLC 25)†‡	Shuttle metabolites	−2.0	2.6	2.6
Vacuolar protein sorting 18 (VPS18)†‡	Ubiquitin (E3) ligase	−4.3	2.0	2.5

*Fold change of differentially regulated transcripts calculated as colonized over uncolonized conditions.
†Transcripts annotated as members of a similar gene family in squid, zebrafish and mouse; squid annotation is shown.
‡Transcripts, either homologs or belonging to a similar gene family, differentially regulated during infections with *Yersinia enterocolitica* [Handley S, Dube P, Miller V (2006) Histamine signaling through the H(2) receptor in the Peyer's patch is important for controlling *Yersinia enterocolitica* infection. *Proc Natl Acad Sci USA* 103:9268–9273.].
§Transcripts annotated as homologs in squid, zebrafish and mouse.

Other Supporting Information Files

Table 4(XLS)
Table 5(XLS)